Aggregation Behavior of Pegylated Bile Acid Derivatives

ARTICLE *in* LANGMUIR · AUGUST 2012

Impact Factor: 4.46 · DOI: 10.1021/la303218q · Source: PubMed

5 AUTHORS, INCLUDING:

Denis Fuentealba
Pontifical Catholic University of Chile
13 PUBLICATIONS **127** CITATIONS
SEE PROFILE

Satu Strandman
Université de Montréal
31 PUBLICATIONS **449** CITATIONS
SEE PROFILE

X. X. Zhu
Université de Montréal
223 PUBLICATIONS **4,785** CITATIONS
SEE PROFILE

Langmuir

Article

pubs.acs.org/Langmuir

Aggregation Behavior of Pegylated Bile Acid Derivatives

Frantz Le Dévédec,[†] Denis Fuentealba,[‡,§] Satu Strandman,[†] Cornelia Bohne,[‡] and X. X. Zhu*[,†]

[†]Department of Chemistry, Université de Montréal, C.P. 6128 succursale Centre-Ville, Montréal, QC, H3C 3J7 Canada

[‡]Department of Chemistry, University of Victoria, P.O. Box 3065 Station CSC, Victoria, BC, V8W 3 V6 Canada

Supporting Information

ABSTRACT: Bile acids are amphiphilic endogenous steroids that act as anionic surfactants in the digestive tract and aggregate in aqueous solutions. Nonionic surfactants were synthesized by grafting poly(ethylene glycol) chains of various lengths (pegylation) to three bile acids (lithocholic, deoxycholic, and cholic acid) using anionic polymerization. The aggregation properties of the derivatives were studied with viscosity measurements and light scattering as well as with steady-state and time-resolved fluorescence techniques, and the aggregates were visualized by transmission electron microscopy to elucidate the effect of pegylation on the aggregation process. The fluorescence results showed a good correlation with the capacity of the bile acid derivatives to solubilize a hydrophobic drug molecule. The solubilization of ibuprofen depends on the length and the number of grafted PEG chains, and the solubilization efficiency increases with fewer PEG chains on the bile acid. The results indicate their potential for use in the design of new bile acid-based drug-delivery systems.

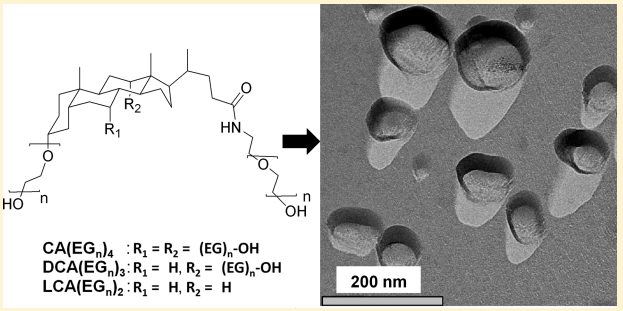

INTRODUCTION

Bile acids are naturally occurring amphiphilic steroids synthesized in the liver of animals and stored in the gallbladder for the emulsification and transport of dietary lipids.[1−3] Their aggregation in aqueous solutions has attracted a great deal of research interest in an effort to understand their interactions with biological membranes, in biliary secretion, and in the solubilization of hydrophobic compounds.[4] The aggregation of bile acids is more complex than that of common ionic surfactants because of their facial amphiphilicity and their incomplete separation of hydrophilic and hydrophobic domains.[3,5−8] They offer a broader critical aggregation concentration (cac) range than conventional surfactants, and the aggregate sizes depend on their concentration because of a continuous aggregation process.[9,10] Bile acids can organize into primary aggregates that form larger secondary aggregates in the shape of prolate ellipsoids or rods.[11,12] They are useful in the solubilization of hydrophobic molecules. It has been suggested that they actually have two types of binding sites—one for hydrophobic molecules and another for relatively hydrophilic molecules—making them adaptable as supramolecular hosts.[13−16] The multiple functional groups of bile acids allow their derivatization to form interesting molecular architectures, such as asymmetric star polymers,[17] molecular pockets,[18,19] and umbrella-like linear−dendritic systems.[20]

Poly(ethylene glycol) (PEG) is the most common nonionic bioacceptable hydrophilic polymer for a number of applications.[21−23] It decreases the aggregation tendency of particles through steric stabilization and is often used to improve the biocompatibility of various systems.[24−26] We introduced four PEG chains to a cholic acid (CA) core, CA(EG_n)$_4$, and showed the dependence of the critical aggregation concentration on the length of the arms.[27] These derivatives can form spherical aggregates in water, providing an encapsulation reservoir for hydrophobic compounds.[17,19]

The number of PEG arms is expected to influence the aggregation properties of the derivatives through steric crowding[27] as well as their interactions with hydrophobic compounds. Therefore, we synthesized a series of pegylated bile acids (BA-PEG) with 2−4 arms composed of 8−17 repeating units of ethylene glycol (EG), CA(EG_n)$_4$, DCA-(EG_n)$_3$, and LCA(EG_n)$_2$ based on cholic acid (CA), deoxycholic acid (DCA), and lithocholic acid (LCA), respectively (Scheme 1). After the critical aggregation concentrations were determined under different conditions, the aggregation properties of the derivatives were studied by dynamic light scattering (DLS) and by steady-state and time-resolved fluorescence spectroscopic methods to understand the effect of pegylation on the aggregation of the bile acids. To gain some understanding of the effect of the length and number of arms on the solubilization of hydrophobic compounds under physiological conditions in view of potential biomedical applications, the solubilization of a model hydrophobic drug, ibuprofen, was also tested in a phosphate buffer solution.

EXPERIMENTAL SECTION

Materials. All chemicals used were purchased from Sigma-Aldrich (Oakville, ON, Canada). Cholic, deoxycholic, and lithocholic acids (all

Received: August 8, 2012
Revised: August 24, 2012
Published: August 27, 2012

Scheme 1. Structure of the Pegylated Bile Acid Derivatives (n = 8−17)

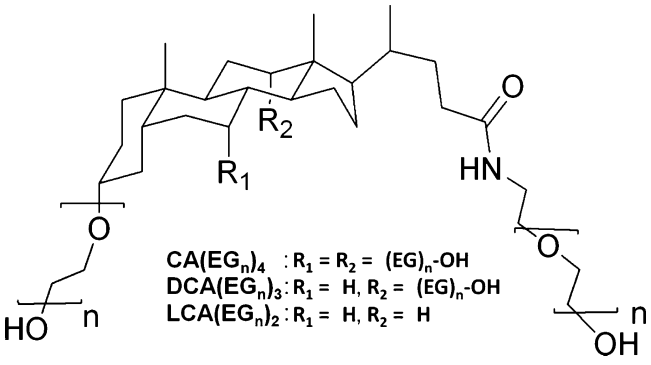

98%), ethylene oxide (99%), ethanolamine (98%), nitromethane (99+ %), and ibuprofen (98%) were used without further purification. Pyrene (99%, Py) was recrystallized twice from ethanol. Methanol (99.8%, spectrograde) and acetonitrile (99.8%, HPLC grade) were obtained from Caledon (Georgetown, ON, Canada) and used as received for fluorescence spectroscopy.

Pegylated bile acids CA$(EG_n)_4$, DCA$(EG_n)_3$, and LCA$(EG_n)_2$ were synthesized by the anionic polymerization of ethylene oxide (EO) on bile acid cores according to a previous report with some modifications.[17] All of the glassware and needles were flame dried under vacuum and purged with argon three times. A typical procedure is the following: A hydroxyethylamide derivative of a bile acid (4 mmol) was placed into a 100 mL flask charged with 40 mL of dry DMSO. Potassium naphthalene solution in THF (0.54 mol/L) was introduced (0.25 equiv) dropwise into the vigorously stirred flask via a cannula by high-pressure argon. Then, dry ethylene oxide chilled in dry ice/acetone was introduced into the flask and polymerized at 40 °C for 48 h. The reaction mixture was neutralized and quenched with concentrated HCl. The DMSO solution was extracted with hexane (three times) to remove naphthalene, and DMSO was removed by distillation under vacuum. A small amount of THF was added to the residue to dissolve the polymer and to precipitate the salt. After the salt was filtered off, the polymer solution was concentrated to dryness by rotary evaporation and high vacuum.

The molar masses of the products were determined by size-exclusion chromatography (SEC), MALDI-TOF mass spectrometry (Figure S1), and ^{1}H NMR spectroscopy (Figure S2), and the results are summarized in Table 1. The degrees of polymerization (number of EG units/arm) calculated from the average values of M_n are indicated. The number of arms was confirmed with end-group analysis by ^{1}H NMR using a reported method (Figure S2).[17] Thermal characteristics of the products were determined by thermogravimetry and differential scanning calorimetry (DSC, Figure S3). The details of the characterization methods are given in the Supporting Information.

Methods. *Aggregation Studies.* Critical aggregation concentrations in water and in phosphate-buffered saline (PBS, pH 7.3, ionic strength 0.1 M) at 25 °C (Table 1) were determined by viscosity measurements on a Cambridge Applied Systems viscometer (model VL-4100). The samples were diluted with milli-Q water to obtain the desired concentrations. Measurements were made five times with an estimated error of 5%. Examples of the viscosity curves are shown in Figure S4.

Dynamic light scattering (DLS) of aqueous samples was performed with a Malvern DLS-Zetasizer Nano ZS instrument equipped with a 4 mW, 633 nm He−Ne laser. Measurements were conducted in backscattering (173°) mode and detected with an Avalanche photodiode. Experiments were repeated seven times at 25 °C. The correlation functions were analyzed by a non-negative least-squares (NNLS) algorithm.

Freeze-fracturing and transmission electron microscopy (TEM) of aqueous solutions of the BA-PEG were performed as described previously.[17] The platinum−carbon replicas were imaged with a FEI Tecnai 12 120 kV transmission electron microscope equipped with a Gatan 792 Bioscan 1k × 1k wide-angle multiscan CCD camera.

Solubilization of Ibuprofen. CA$(EG_n)_4$, DCA$(EG_n)_3$, and LCA-$(EG_n)_2$ solution samples (20−40 mM) were prepared in PBS. Briefly, BA-PEGs and ibuprofen (20 mg) were dissolved in 1 mL of methanol. After the complete evaporation of the solvent under vacuum, PBS was added. The solutions were sonicated for 5 min and placed at a chosen temperature under stirring for 18 h of equilibration. After the solutions were centrifuged for 20 min at 1.04g and the supernatant was filtered (0.8 μm nylon filter), the amount of solubilized ibuprofen in the supernatant was determined by high-performance liquid chromatography (HPLC).[28] FT-IR spectra of BA-PEG, ibuprofen, and their mixture prior to the addition of PBS are presented in Figure S5.

The solubilization of ibuprofen by the BA-PEG aggregates in aqueous solutions is determined by two factors: the molar solubilization capacity (χ) and the micelle−water partition coefficient (K). Unlike χ, K depends on the solubility of the compound in water. To eliminate the surfactant concentration dependence of K, a molar micelle−water partition coefficient K_M is introduced as

$$\chi = \frac{S_{tot} - S_w}{C_{surf} - cac}, \quad K_M = \frac{\chi(1 - cac)}{S_w} \tag{1}$$

where S_{tot} is the total amount of ibuprofen solubilized by the surfactant, S_w is the solubility of ibuprofen in water, C_{surf} is the concentration of BA-PEG, and cac is the critical aggregation concentration of BA-PEG. Thermodynamically, the solubilization can be considered to be a normal partitioning of the drug between two phases (i.e., inside and outside the micellar aggregates). Hence, the standard free energy of solubilization (ΔG_s°) can be expressed as

$$\Delta G_s^0 = -RT \ln K_M \tag{2}$$

Photophysical Studies. Sample Preparation. The BA-PEG samples (n = 8, 9) were dissolved in deionized water from a nanopure

Table 1. Properties of Pegylated Bile Acids

BA-PEG[a]	M_n (g/mol) SEC (PDI)[b]	M_n (g/mol) ^{1}H NMR	M_n (g/mol) MALDI-TOF	EG units/arm[c]	T_g (°C)[d]	T_m (°C)[e]	cac (mm)[f]
CA$(EG_8)_4$	1450 (1.07)	2210	2100	8	−58	22	13
DCA$(EG_9)_3$	1370 (1.06)	1690	1750	9	−58	12	12
LCA$(EG_9)_2$	1130 (1.06)	980	1420	9	−56	−3	16
CA$(EG_{16})_4$	3070 (1.10)	3360	3080	16	N/O	31	16
DCA$(EG_{17})_3$	2640 (1.10)	2940	2710	17	−58	27	15
LCA$(EG_{16})_2$	1630 (1.05)	1950	1960	16	−62	15	11

[a]CA, DCA, and LCA refer to cholate, deoxycholate, and lithocholate, respectively. The subscripts refer to the degree of polymerization and the number of PEG arms. [b]Number-average molar mass (polydispersity index) from SEC calibrated with PEG and PS standards. [c]Degree of polymerization of individual arms calculated from the average values of M_n. [d]Glass-transition temperature T_g determined by DSC. [e]Melting point T_m determined by DSC. [f]Critical aggregation concentration determined by dynamic viscometry in pure water at 25 °C (error ±1 mm, five measurements per concentration).

dx.doi.org/10.1021/la303218q | Langmuir 2012, 28, 13431−13440

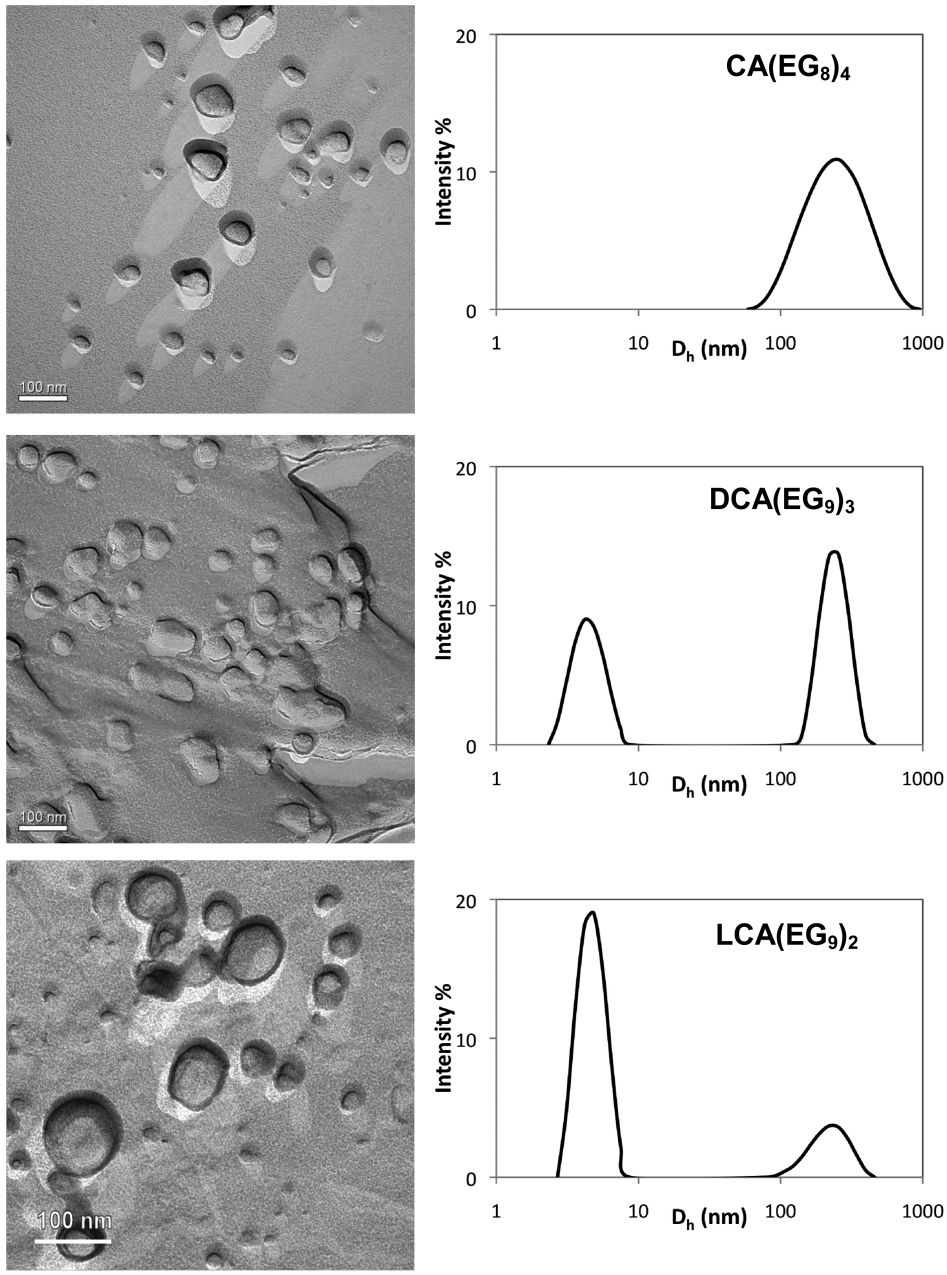

Figure 1. TEM micrographs of freeze-fractured samples (left) and distributions of hydrodynamic diameters (right) for 30 mM aqueous solutions of BA-PEGs determined at a backscattering angle of $\Theta = 173°$, from top to bottom: $CA(EG_8)_4$, $DCA(EG_9)_3$, and $LCA(EG_9)_2$. The scale bars in the micrographs are 100 nm.

Sybron Barnstead system and were shaken for 1−3 h. The solutions were then filtered through a 0.45 μm nylon syringe filter. The samples containing Py were prepared by injecting a small aliquot of a Py stock solution in methanol (2 mM) into an aqueous solution of BA-PEG and shaken overnight (0.5% methanol added). The final concentrations for BA-PEG were set in order to work below (5 mM) and above (20 mM) the cac's of the samples. For the quenching experiments, a stock solution of nitromethane (1 M) was prepared in acetonitrile and injected directly into 3.0 mL of the BA-PEG solutions containing Py. The amount of acetonitrile added to the solutions was less than 1%.

Absorption Spectra and Steady-State Fluorescence. Absorption spectra were recorded on a Varian Cary 1 spectrophotometer at room temperature using 10 mm path length cells. The absorption of a reference cell with deionized water was subtracted from the absorption of the samples. The fluorescence emission spectra were measured on a PTI QM-2 fluorimeter at 20.0 ± 0.1 °C using 2 mm × 10 mm fluorescence cells. The excitation wavelength was 331 nm, and the emission was collected from 350 to 550 nm. The bandwidths for the excitation and emission monochromators were 1 nm. Because of the high absorbance of the BA-PEG samples (Figure S6) in the region where Py fluoresces, the actual path length for the detection of the fluorescence was kept short (~1 mm) to minimize any self-absorption of the emission by the samples (control experiments in the SI). The emission from control solutions in the absence of Py was subtracted from the emission of the samples.

Time-Resolved Fluorescence. Time-resolved fluorescence measurements were performed with an OB920 single-photon counting system from Edinburgh at 20.0 ± 0.1 °C using 10 mm × 10 mm fluorescence cells. The excitation source was a 335 nm light-emitting diode (EPLED-330, Edinburgh). The stop rate was less than 1% of the start rate, and the repetition rate for the light pulses was 0.2 or 0.5 MHz. The decays were collected for 10 000−20 000 counts in the channel of maximum intensity. The time window for the collection was 1 or 2 μs.

dx.doi.org/10.1021/la303218q | *Langmuir* 2012, 28, 13431−13440

The instrument response function (IRF) was collected by scattering the light at 335 nm with a dilute Ludox solution. The fluorescence lifetimes were obtained by fitting the decays to a sum of exponential functions according to eq 3, where A_i is the pre-exponential factor and τ_i is the fluorescence lifetime for each species. The pre-exponential factors are related to the relative concentration of each emissive species. The reconvolution of the IRF with the calculated fit was not performed because the IRF was very narrow on the time scale used. Instead, a tail-fitting routine from the FAST Edinburgh software was used to fit the decays. The quality of the fits was evaluated from the randomness of the residuals and a χ^2 value in the range of 0.9−1.2.[29]

$$I(t) = \sum_{1}^{i} A_i e^{-t/\tau_i} \tag{3}$$

The presence of fluorescence impurities in the BA-PEG samples was observed as a fast decay after the light pulse and was confirmed in control experiments in the absence of Py. The lifetimes for these impurities are much shorter than the lifetimes for Py, and the impurity lifetimes were fixed for the analysis of the Py lifetime (Figures S7 and S8; details in the Supporting Information).

The quenching of the Py fluorescence in the presence of BA-PEG by nitromethane was studied. The quenching rate constant (k_q) for the fluorescence was obtained by analyzing the shortening of the Py fluorescence lifetime (τ) at increasing concentrations of the quencher (Q) according to eq 4, where τ_0 corresponds to the fluorescence lifetimes of Py in the absence of the quencher.

$$\frac{1}{\tau} = \frac{1}{\tau_0} + k_q[Q] \tag{4}$$

The analysis of the time-resolved quenching data (Figure S9 in the Supporting Information) is complex because of the presence of multiple fluorescent species. The fluorescence decays were analyzed with the FAST software from Edinburgh, which allows the fitting of the data to a maximum of four exponentials. Considering that the impurities in the BA-PEG samples show two lifetimes, the maximum number of lifetimes that can be recovered for Py is two. One of these Py lifetimes was fixed to the value for Py in water in the absence and presence of nitromethane (details in Supporting Information).

RESULTS

Aggregation of BA-PEGs. Because of the complex aggregation behavior of bile acids and bile salts, the aggregation transition occurs over a wide concentration range. Therefore, the critical aggregation concentrations (cac's) vary greatly and often depend on the method of determination. The attachment of PEG chains alters the aggregation characteristics of bile acids by increasing the steric repulsion and decreasing the direct interactions between the hydroxyl groups. The cac values of the BA-PEG samples, determined by dynamic viscometry experiments and shown in Table 1, are in good agreement with those determined earlier for pegylated cholic acid by surface tensiometry.[17] Millimolal (m*m*) concentration (1 mmol of solute per 1 kg of solvent) was used because of its convenience in the calculation of concentration for samples of varying volume but known weight. At low concentrations, the molal and molar (1 mol of solute per 1 L of solvent) concentrations are similar in value. For comparison, some of the reported cac's for cholates, deoxycholates, and lithocholates are 9−18, 5−10, and 0.9 mM, respectively.[30] Hence, pegylation has the highest solubilizing effect on lithocholate. The viscosity curves of BA-PEGs with n = 8−17 (number of ethylene glycol units per arm) suggest a broader aggregation transition for the BA-PEGs with shorter PEG chains (Supporting Information). This may stem from their higher hydrophobicity and thus higher tendency toward secondary aggregation. Electrolytes at low concentration, such as in PBS, have only a minor effect on the cac (±2 m*m*) because BA-PEGs can be considered to be nonionic surfactants.

Both dynamic light scattering results and TEM images of the carbon replicas prepared by the freeze-fracture method for the aqueous solutions of BA-PEGs (20−70 mM) indicate the polydisperse nature of the aggregates above the cac. The micrographs show spherical aggregates of variable sizes, part of which seem to be composed of fused smaller spheres (Figure 1), and the aggregates of native bile salts are known to be rodlike, in accordance with our previous observations.[17] In DLS, Laplace inversion algorithms such as the non-negative least-squares algorithm (NNLS) used in the analysis of autocorrelation functions of scattered light are known to fail in some cases, for instance, when the size distributions are broad, because of the ill-conditioned problem of fitting, leading to bimodal size distributions.[31] Therefore, the intensity-weighted size distributions can be either bimodal or broad and monomodal even for the same sample. Thus, several parallel experiments have been conducted, giving an average distribution for each sample. In addition, light scattering emphasizes large scatterers, and hence the size distributions obtained by DLS do not correspond to the distribution of aggregate sizes observed in the micrographs. It is to be noted that the absence of peaks with a small D_h value for the sample does not rule out the presence of small aggregates, which may not be detectable because of the presence of larger scatterers. The mean hydrodynamic diameters corresponding to the fast diffusion mode (D_{hf}) in bimodal distributions were in the range of 4.2−4.7 nm. For comparison, D_h values of primary aggregates of bile salts determined by DLS have been reported to be 2.0−3.4 nm.[9] Hence, the fast diffusion mode could also refer to the presence of small BA-PEG aggregates that are not visible in the micrographs. The average hydrodynamic diameters from the intensity-weighted size distributions by DLS corresponding to the slow diffusion mode (D_{hs}) at 30 mM were 352 ± 109 nm for the EG_{16-17} series and 206 ± 24 nm for the EG_{8-9} series (Figure 1). Increasing the concentration of the BA-PEGs broadens the size distributions, and added salt (PBS solution) induces further aggregation of the less hydrophilic BA-PEGs. Although $CA(EG_8)_4$ showed no effect, $DCA(EG_9)_3$ showed a 1.5-fold increase and $LCA(EG_9)_2$ showed a 2.5-fold increase in D_{hs} in PBS compared to that of the salt-free solutions. This suggests that the aggregates of the most hydrophilic BA-PEGs should be stable at physiological pH and ionic strength.

Solubilization of Ibuprofen. Ibuprofen is a common poorly water-soluble nonsteroidal anti-inflammatory drug (Scheme 2, logarithmic octanol−water partition coefficient log P = 3.6), which was selected as a model compound for the solubilization studies.[32] The solubilization requires breaking the crystal lattice of the ibuprofen, enhanced by favorable interactions between the drug and the solubilizing agents, in this case BA-PEGs. This was confirmed by X-ray diffraction experiments of the mixtures of ibuprofen and $CA(EG_8)_4$ at different mixing ratios, showing the disappearance of the peaks

Scheme 2. Chemical Structure of Ibuprofen

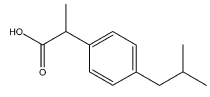

dx.doi.org/10.1021/la303218q | Langmuir 2012, 28, 13431−13440

of crystalline ibuprofen indicating an amorphous state (data not shown). The interactions were further confirmed by the DSC results, which showed an increase in the melting point and a decrease in the crystallization temperature of $CA(EG_8)_4$ with an increasing amount of ibuprofen (data not shown). Good mixing is evidenced by FT-IR spectra of ibuprofen showing a shift in the C═O group stretching vibration from 1708 to 1732 cm^{-1} and in the aromatic C−C group stretching of ibuprofen from 1502 to 1513 cm^{-1}, suggesting the hydrophobic interactions of the aromatic ring of ibuprofen with the steroid core of the bile acid (Figure S5).

During solubilization, ibuprofen may interact with different sites on the BA-PEGs. The drug could be absorbed at the interface between the aggregate surface and the aqueous phase, or it may interact with the PEG chains or with the inner core of the pegylated derivatives. The solubilization parameters include a molar solubilization capacity (χ), a molar micelle−water partition coefficient K_M, and the standard free energy of solubilization ΔG_s° for the solubilization of ibuprofen by BA-PEG in PBS. These parameters are calculated from the concentration dependence of the solubilized drug (Figure 2)

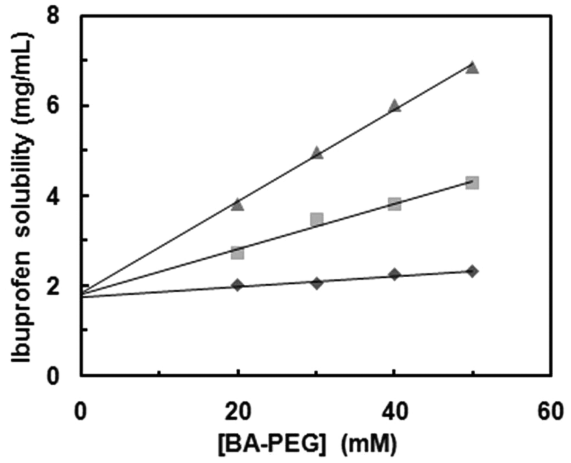

Figure 2. Solubilization of ibuprofen by the pegylated bile acid derivatives $CA(EG_8)_4$ (♦), $DCA(EG_9)_3$ (■), and $LCA(EG_9)_2$ (▲). The concentrations of ibuprofen were determined by HPLC after 18 h of equilibration in PBS (pH 7.3) at 25 °C. The average error of three individual experiments for each concentration is less than 5% (±0.2 mg/mL).

through eqs 1 and 2, and the results are presented in Table 2. The amount of solubilized ibuprofen and negative ΔG_s° follow

Table 2. Solubilization Parameters for BA-PEGs[a]

BA-PEG	ibuprofen solubility (mg/mL)[b]	χ	K_M	ΔG_s° (kJ/mol)
$CA(EG_8)_4$	2.8	32	17	−7.0
$DCA(EG_9)_3$	4.4	88	45	−9.5
$LCA(EG_9)_2$	6.1	172	89	−11.1
$CA(EG_{16})_4$	2.2	13	7	−4.7
$DCA(EG_{17})_3$	3.9	77	40	−9.1
$LCA(EG_{16})_2$	6.0	143	74	−10.7

[a]Molar solubilization capacity (χ), molar micelle−water partition coefficient (K_M), and thermodynamic parameter (ΔG_s°) of ibuprofen solubilized by BA-PEGs (40 mM). [b]The solubilities of ibuprofen in the presence of BA-PEG were determined by HPLC from three individual experiments with an average error of less than ±0.2 mg/mL.

the order LCA > DCA > CA, indicating that the spontaneous formation of micellar aggregates by the star polymers bearing more PEG arms is thermodynamically less favored and that the solubilizing power of these star polymers also shows a decrease. Linear regression gives a solubility of free ibuprofen of 1.9 mg/mL in PBS at pH 7.3 (data not shown). The same value was obtained by determining the solubility of ibuprofen in buffer by HPLC in the absence of BA-PEGs.

The most hydrophobic BA-PEG is the most efficient at solubilizing the drug, over a range similar to that of nonionic $C_{12}EO_8$ surfactant (*n*-dodecyl octa(ethylene oxide)) and Tween surfactants (i.e., between 5 and 8 mg/mL ibuprofen).[33] The solubilization of a hydrophobic compound by the Tween surfactants depends on the compound's cac and hydrophilic−lipophilic balance (HLB). The HLB is defined by a number that ranges typically from 0 to 20. In general, an HLB number of <10 indicates that the surfactant has low solubility in water, and an HLB number of between 10 and 20 indicates good water solubility. Surfactants with lower HLBs tend to have a greater capacity for the encapsulation of hydrophobic compounds.[28] The HLB values of BA-PEGs are expected to be similar to that of sodium cholate (HLB = 18)[34] or those of Tween surfactants (HLB = 11−17 for Tweens with 20 EG units).[34,35]

Fluorescence Studies. *Time-Resolved Fluorescence.* Py is a useful fluorescence probe for studying the properties of the microenvironment of complex systems.[28,36,37] The fluorescence lifetime of Py usually increases upon its incorporation into a host system, and the shape of its fluorescence emission spectrum is diagnostic of the polarity of the microenvironment.[36,38−40] Because the apparent average hydrodynamic diameters of the slow diffusion mode (D_{hs}) of BA-PEGs with n = 8 to 9 do not vary greatly but there is a large difference in the solubilization capacities of ibuprofen, this series of compounds was selected for fluorescence studies. To study the incorporation of Py (logarithmic octanol/water partition coefficient log P = 5.2)[41] into the BA-PEG aggregates, we have used mainly time-resolved fluorescence measurements complemented with steady-state fluorescence measurements. The aqueous solutions of BA-PEGs show high absorption at around 300 nm extending far into the visible region. Control experiments in the absence of Py showed the presence of multiple fluorescence impurities with lifetimes shorter than 10 ns (Table S1). These lifetimes are very short when compared to the lifetime for excited Py (>60 ns), which makes it possible to distinguish between the impurities and Py emission in the kinetic experiment. It is worth noting that no impurities were observed in the NMR spectra, suggesting that the amount of impurities is low but their fluorescence efficiency is significant.

The fluorescence decay of Py in an aqueous solution of $LCA(EG_9)_2$ (Figure 3) fit the sum of four exponentials well. Two short lifetimes (<10 ns) were assigned to the impurities in the sample, whereas the two longer lifetimes (>60 ns) were assigned to different Py species. The short lifetimes were constant for different BA-PEG concentrations and were fixed for the analysis of the decays in the presence of Py. The relative contributions of the Py species to the fluorescence decay have been evaluated from the pre-exponential factors (eq 3). The A values have been calculated by taking into account only the pre-exponential factors for the Py species and normalizing the sum of these A values to 1. The lifetime of the minor Py species (A = 0.05 ± 0.01) could be fixed to the lifetime of Py in water (130 ns),[37,42,43] and the major longer-lived Py species (A = 0.95 ± 0.01) was assigned to Py inside the $LCA(EG_9)_2$ aggregates. If

dx.doi.org/10.1021/la303218q | *Langmuir* 2012, 28, 13431−13440

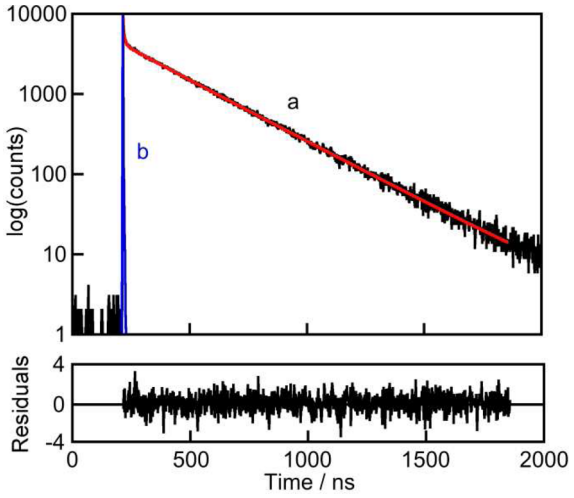

Figure 3. Fluorescence decay for Py (2 μM) in 5 mM aqueous solutions of LCA$(EG_9)_2$. The decay is shown in black (a), the IRF is shown in blue (b), and the fit is shown in red. The lifetimes for the impurities (2 and 8 ns) and Py in water (130 ns) were fixed. The recovered fourth lifetime was 286 ns (χ^2 = 0.998). The residuals for the fit are shown in the bottom panel.

the lifetime of the shorter-lived Py species was not fixed to the lifetime of Py in water, the residuals between the experimental data and the fit and the lifetime of the long-lived component did not change significantly. Similar results were observed for DCA$(EG_9)_3$. In the case of CA$(EG_8)_4$, the lifetime of the shorter-lived Py species could not be fixed to the lifetime of Py in water and a lifetime of ~60 ns was recovered from the fits at different concentrations (Figure S8).

For all of the samples, the fluorescence lifetime of Py increased significantly upon its incorporation into the BA-PEGs in aqueous solution (Table 3). The lengthening of the lifetime is likely related to the protection of the Py molecule from oxygen in solution and/or to the lower polarity of the microenvironment in which the molecule is incorporated.[36,38] When the A values for the long-lived component (τ_1) are compared at a concentration of 5 mM for the different BA-PEGs, a decrease in the order LCA$(EG_9)_2$ > DCA$(EG_9)_3$ > CA$(EG_8)_4$ is observed, indicating a decreasing amount of incorporated Py with an increasing number of PEG arms. A similar trend is observed at a concentration of 20 mM, although no difference in the A values can be observed between LCA$(EG_9)_2$ and DCA$(EG_9)_3$ at this concentration because all Py is incorporated in the aggregates. This result suggests that the number of PEG arms plays an important role in the binding of hydrophobic molecules, as is also shown by the ibuprofen solubilization studies described above. At low BA-PEG concentrations (5 mM, Table 3), the A values of the long-lived component indicate that some Py was incorporated in all BA-PEGs. When the concentration of BA-PEG was higher (20 mM), the A values of the long-lived component increased, consistent with the incorporation of more Py into the aggregates. The lifetime of the longer-lived Py species does not change significantly with the sample concentration for LCA$(EG_9)_2$ and DCA$(EG_9)_3$, suggesting that the aggregates do not change upon increasing the concentration of BA-PEG. The lengthening of the Py lifetime observed at the higher concentrations of CA$(EG_8)_4$ suggests that the structure of the Py binding site in the aggregate may change when the concentration of this compound was increased.

Table 3. I/III Ratios, Fluorescence Lifetimes (τ_i), and Pre-Exponential Factors (A_i) of Py (2 μM) in the Presence of 5 and 20 mM Aqueous BA-PEG Solutions[a]

BA-PEG	[BA-PEG] (mM)	I/III ratio	τ_1 (ns) (A_1)	τ_2 (ns) (A_2)
LCA$(EG_9)_2$	5	1.33 ± 0.01	283 ± 3 (0.95 ± 0.01)	130^{fixed} (0.05 ± 0.01)
	20	1.32 ± 0.01	280 ± 1 (1)	
DCA$(EG_9)_3$	5	1.34 ± 0.02	274 ± 1 (0.81 ± 0.01)	130^{fixed} (0.19 ± 0.01)
	20	1.20 ± 0.03	265 ± 1^b (1)	
CA$(EG_8)_4$	5	1.49 ± 0.02	181 ± 1 (0.70 ± 0.01)	57 ± 4 (0.30 ± 0.01)
	20	1.40 ± 0.01	215 ± 2 (0.86 ± 0.01)	60^{fixed} (0.14 ± 0.01)

[a]The errors in the lifetimes and the A values correspond to the average errors from two independent experiments. The lifetimes for the impurities were fixed to the average values obtained from independent measurements (Table S1). [b]The lifetimes of the impurities for this sample were fixed to 2.1 and 10 ns.

Steady-State Fluorescence: Polarity of the Microenvironment. The polarity of the microenvironment inside the BA-PEG aggregates can be estimated from the ratio of the intensities for emission bands I (~370 nm) and III (~382 nm) in the Py fluorescence spectrum (Figure S10). The I/III ratios for common solvents range from 0.5 to 0.6 for aliphatic nonpolar solvents and from 1.6 to 1.9 for water.[39,40,44,45] The high absorption of the impurities in BA-PEG samples could potentially alter the Py emission intensity because of self-absorption and modify the relative intensities of bands I and III. The control experiment described above and in the Supporting Information showed that self-absorption did not alter the I/III ratios.

The interpretation of the I/III ratios is straightforward when a single Py species is present in the medium. In the presence of a host system when a fraction of Py is located in water and another fraction is bound to the host, the I/III ratio corresponds to the contribution of each Py species, taking into account the relative concentrations of these species. Increasing the concentration of BA-PEG led to a decrease in the I/III ratios of all samples (Table 3) because of the higher fraction of Py bound to the aggregate. A single lifetime for the excited state of Py was observed with 20 mM LCA$(EG_9)_2$ and DCA$(EG_9)_3$, indicating that all of the Py molecules were bound to the aggregates. The I/III ratios obtained for these BA-PEGs were 1.32 ± 0.01 and 1.20 ± 0.03, respectively (Table 3), representing the polarity of the microenvironment sensed by Py inside the aggregates. As a reference, the I/III ratios for Py in methanol and ethanol are 1.35 and 1.18, respectively,[39] indicating that the polarity inside the aggregates is similar to that of these solvents. In the case of CA$(EG_{10})_4$, two lifetimes were observed for Py even at 20 mM BA-PEG concentration. Therefore, the I/III ratio obtained at 20 mM CA$(EG_8)_4$ (1.40 ± 0.01) can be taken as the upper limit for the polarity sensed by Py inside the aggregates of CA$(EG_8)_4$, being similar to the polarity of ethyl acetate (I/III ratio = 1.37).[39] As a comparison, the I/III ratios for Py in bile salt aggregates are in the range of 0.66 to 0.86 for sodium cholate and deoxycholate,[42,43,46−48] and a number of literature values have been summarized elsewhere.[49] These reported I/III ratios for bile salt aggregates in aqueous solution are much lower than the I/III ratios observed

for the BA-PEG derivatives used in this study, indicating that the polarity in the BA-PEG aggregates is higher than that sensed by Py in the aggregates of the parent bile salts.

Fluorescence Quenching Studies: Accessibility of Molecules from the Aqueous Phase to Py in the Aggregates. The accessibility of molecules from the aqueous phase to the interior of aggregates can give information on the structure of the aggregates. Therefore, quenching studies with nitromethane were performed using time-resolved fluorescence. The fluorescence decay is usually fast compared to the time scale of the association/dissociation dynamics of the guest with the host; therefore, the guest molecule can be considered to be stationary during fluorescence emission. Under these conditions, the quenching of the excited state reflects the accessibility of the quencher molecule to the guest−aggregate complex.[36] This assumption requires that the quenching rate constant be diffusion-controlled. Otherwise, the changes in the quenching rate constant could reflect the changes in the intrinsic reactivity caused by the differences in the environment of the fluorophore. The quenching rate constant for Py by nitromethane in water was determined in previous work[42] to be $(7.1 \pm 0.2) \times 10^9$ M^{-1} s^{-1}, which is close to the rate constant of a diffusional process (6.5×10^9 M^{-1} s^{-1} at 20 °C).[50] Quenching studies were performed at a BA-PEG concentration of 5 mM for $LCA(EG_9)_2$ and $DCA(EG_9)_3$ to reduce the amount of impurities present in the solutions. For $CA(EG_8)_4$, a concentration of 20 mM was used to maximize the contribution of bound Py to the fluorescence decay and to recover the Py lifetimes with better precision.

The two long lifetimes assigned to Py species were shortened in the presence of nitromethane for all of the BA-PEG samples. At a high concentration of nitromethane (10 mM), the calculated lifetime for Py in water was very short and was comparable to the lifetimes of the impurities for BA-PEGs. The lifetime of Py inside the aggregates was also significantly shortened. Another longer-lifetime component in the emission of Py can be observed for $LCA(EG_9)_2$, suggesting the presence of a third minor Py component, which cannot be observed for $DCA(EG_9)_3$. The lifetime for this additional component could not be analyzed because the maximum number of lifetimes that can be recovered with the fitting software is four. In the case of $CA(EG_8)_4$, an additional well-protected component became available (Table S2), suggesting that at the higher concentration for this BA-PEG different aggregates can be formed. The investigation of the polydispersity of aggregation is beyond the scope of the current work and was not pursued further.

The quenching rate constants for Py in the BA-PEG aggregates by nitromethane were calculated from the slopes of the quenching plots (Figure 4) according to eq 4, and the results are summarized in Table 4. The lifetimes analyzed in the quenching plots are those assigned to Py in the aggregate. The quenching rate constants for Py increase in the order $LCA(EG_9)_2$ < $DCA(EG_9)_3$ < $CA(EG_9)_4$, indicating better access of the quencher to the aggregates and thus a lower protection of Py inside the aggregates with increasing number of PEG arms. This protection efficiency can also be described by the ratio of the quenching rate constants in water and in the presence of the BA-PEG aggregates shown in Table 4.

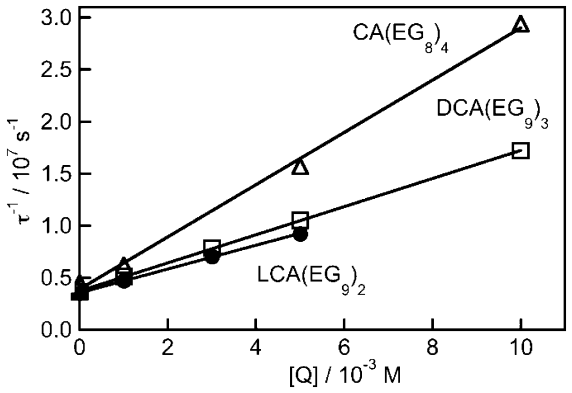

Figure 4. Quenching of the singlet excited state of Py (2 μM) by nitromethane in an aqueous solution of 5 mM $LCA(EG_9)_2$, 5 mM $DCA(EG_9)_3$, and 20 mM $CA(EG_8)_4$.

Table 4. Quenching Rate Constants (k_q) for Py (2 μM) in the Presence of 5 mM $LCA(EG_9)_2$, 5 mM $DCA(EG_9)_3$, and 20 mM $CA(EG_8)_4$ in Aqueous Solution Quenched with Nitromethane[a]

BA-PEG	$k_q^{BA\text{-}PEG}/10^9$ M^{-1} s^{-1}	$k_q^{water}/k_q^{BA\text{-}PEG}$
$LCA(EG_9)_2$	1.16 ± 0.02	6.1 ± 0.2
$DCA(EG_9)_3$	1.42 ± 0.06	5.0 ± 0.2
$CA(EG_8)_4$	2.5 ± 0.3	2.8 ± 0.4

[a]The errors correspond to the propagation of errors from two independent experiments.

DISCUSSION

PEG is a common polymer used for the modification of molecules intended to be employed in biological systems. PEG substituents enhance the hydrophilicity of molecules, improving their biocompatibility and also providing the ability for further functionalization with cellular recognition sites. Bile acids are naturally occurring compounds that form aggregates in solution. Aggregation occurs continuously,[9,10] and binding sites with different properties are available that bind molecules with different hydrophobicities. Bile acid aggregates were shown to act as adaptable host systems where the structure and properties of the guest−host complex change depending on the shape and structure of the guest.[14,51] The adaptable nature of these aggregates has been exploited to solubilize functional guests, such as aqueous insoluble photochromic compounds,[52] without inhibiting their activity. Bile acid aggregates have the potential to act as drug-delivery systems with the advantage that they are more structured than conventional micelles but also more adaptable than rigid hosts, such as macrocycles. PEG incorporation into bile acids was shown to affect the cac, and the formed aggregates are spherical.[17] The objective of this work was to characterize the aggregates of BA-PEGs further, including the properties of the binding sites and the solubilization efficiency of the different bile acid star polymers for a relatively hydrophobic model drug, ibuprofen.

The number and length of the PEG chains were varied to probe how these parameters affect the aggregation of the BA-PEGs. The number of PEG chains or the increase in their length did not significantly affect the cac values, which range from 11 to 16 mM for the three BA-PEGs. The same cac range was observed for the aggregates in PBS, showing that aggregation occurs in the same concentration range in a biologically relevant buffer. The range for the cac's of the BA-PEGs is much narrower than that determined for the native bile salts (9−18 mM for cholates, 5−10 mM for deoxycholates, and 0.9 mM for lithocholates).[30] In the case of native bile salts, the

dx.doi.org/10.1021/la303218q | *Langmuir* 2012, 28, 13431−13440

number of hydroxyl groups defines the hydrophobicity of the bile salt monomer, and a decrease in the number of hydroxyl groups has a large effect on the cac. In the case of BA-PEGs, the PEG chains provide larger hydrophilic moieties and the effect of the number of PEG chains is smaller than the effect of the number of hydroxyl groups in the native bile salts. In addition, in the case of native bile salts the head groups are negatively charged and aggregation corresponds to a balance between the attractive interactions of the hydrophobic portions of the molecules and the repulsive interactions between the head-groups. The BA-PEGs are neutral; therefore, an increase in the hydrophobic fraction of the molecule by removing a PEG chain will have a smaller effect on the cac. It is important to note that BA-PEGs, in contrast to native bile salts, can be used in acidic solutions because there is no protonation site, which for the native bile salts leads to low solubility of the monomers at low pH.

The polarity of the binding site in the BA-PEGs was inferred from the I/III intensity ratios of the pyrene emission spectra. The polarity is higher for the BA-PEGs (I/III = 1.2−1.4) than observed for the primary aggregate of native bile salts (0.66−0.86).[42,43,46−48] The pyrene singlet excited-state lifetimes in BA-PEG aggregates were lengthened, with a longer lifetime being observed for pyrene bound to $LCA(EG_9)_2$ and $DCA(EG_9)_3$ aggregates (265−283 ns) than for pyrene in $CA(EG_8)_4$ aggregates (181−215 ns). The shorter lifetime in the case of $CA(EG_8)_4$ suggests that the binding site in this BA-PEG aggregate is somewhat different from the binding site in the other two aggregates. The pyrene lifetimes in BA-PEG are substantially shorter than observed in sodium cholate (340 ns)[43] or sodium taurocholate (317 ns)[53] aggregates. The structure of the BA-PEG aggregates is not known and may not include the primary aggregates that are the binding sites for pyrene in the aggregates of the native bile salts. The more polar binding sites in the BA-PEGs and the shorter lifetimes for excited pyrene suggest a less-rigid environment in the BA-PEG aggregates than in those of sodium cholate or taurocholate. These properties are important for a drug delivery system because most drugs contain heteroatoms and are more hydrophilic than a polyaromatic hydrocarbon such as pyrene.

The formation of more accessible binding sites in the BA-PEG aggregates than observed for the native bile salts is supported by the analysis of the nitromethane quenching rate constants for the singlet excited state of pyrene bound to the aggregates. These quenching rate constants are a measure of the access of the quencher to the excited guest inside the aggregate. In the case of native bile salts, these quenching rate constant are on the order of 10^8 M^{-1} s^{-1},[42,54] which are one order of magnitude lower than the quenching rate constants observed for Py bound to BA-PEG aggregates, showing that for the BA-PEG aggregates the access of nitromethane to the interior of the aggregate is more facile. The quenching rate constant is highest for $CA(EG_8)_4$ and lowest for $LCA(EG_9)_2$, suggesting that the accessibility to the aggregate is lower for the more hydrophobic BA-PEG, which also contains the smallest number of PEG chains. This result is in line with the lifetimes and I/III ratio measurements discussed above and supports the assignment that the binding sites for these three aggregates are somewhat different.

Ibuprofen was used as a model for a drug molecule because it is not very hydrophobic. The solubilization efficiency in the BA-PEG aggregates is the lowest for $CA(EG_8)_4$, with $DCA(EG_9)_3$ having an intermediate value and the highest solubilization being observed for $LCA(EG_9)_2$. This trend is in agreement with the quenching rate constants for bound pyrene, suggesting that pyrene is probing the same environment to which ibuprofen binds. The solubilization trend observed for ibuprofen suggests that in developing a drug-delivery system it will be important to balance the water compatibility of the host carrier with the hydrophobicity and compactness of the binding site. Finally, it is important to emphasize that the ibuprofen/BA-PEG system is amorphous, which is advantageous when considering BA-PEGs as potential drug-delivery systems because the formation of polymorphs can be prevented.

■ CONCLUSIONS

Pegylated bile acids can form spherical aggregates that are capable of encapsulating hydrophobic compounds in aqueous solutions, as demonstrated with ibuprofen in this study. Their encapsulation efficiency depends on the length and number of attached PEG chains and therefore the choice of the bile acid core (cholic, deoxycholic, or lithocholic acid). The solubilization studies and fluorescence experiments indicate an enhanced incorporation of the relatively hydrophobic ibuprofen by BA-PEG with a fewer number of PEG arms. The results also suggest that the steric crowding by PEG chains may result in a more hydrophilic and less protected environment inside the aggregates. Clearly, this family of bile acid derivatives has the potential to be used as drug carriers. Even though the solublization efficiency is an important factor, whether BA-PEGs with fewer PEG chains have an overall better performance as a drug carrier remains to be answered by additional experiments. The biocompatibility and the stability of the micellar aggregates should be addressed to provide a more complete assessment of these pegylated star polymers.

■ ASSOCIATED CONTENT

Ⓢ Supporting Information

^{1}H NMR and MALDI-TOF spectra. DSC thermograms and cac determination of the pegylated bile acids. FT-IR spectra of the BA-PEG/ibuprofen mixtures. Absorption spectra of BA-PEGs. A description of the control experiments for the reabsorption of emission. Fluorescence lifetime data. Steady-state emission spectrum of Py in the presence of BA-PEGs. Data of the quenching experiments. This material is available free of charge via the Internet at http://pubs.acs.org.

■ AUTHOR INFORMATION

Present Address

[§]Laboratorio de Química Biológica, Facultad de Química, Pontificia Universidad Católica de Chile, Santiago, Chile.

Notes

The authors declare no competing financial interest.

■ ACKNOWLEDGMENTS

We thank Drs. Jeannie Mui, S. Kelly Sears, and Hojatollah Vali at McGill University for their help with the freeze-fracture technique and transmission electron microscopy. The NSERC of Canada, FQRNT of Quebec, and the Canada Research Chair program are acknowledged for financial support. The authors of U de M are members of CSACS funded by FQRNT and GRSTB funded by FRSQ.

REFERENCES

(1) Arias, I. M.; Boyer, J. L.; Fausto, N.; Jakoby, W. B.; Schachter, D. A.; Shafritz, D. A. In *The Liver: Biology and Pathobiology*, 3rd ed.; Carey, M. C.; Duane, W. C., Eds.; Raven Press: New York, 1994.

(2) Hofmann, A. F.; Small, D. M. Detergent Properties of Bile Salts: Correlation with Physiological Function. *Annu. Rev. Med.* **1967**, *18*, 333−376.

(3) Small, D. M.; Nair, P. P.; Kritchevsky, D. *The Bile Acids; Chemistry, Physiology and Metabolism*: Plenum Press: New York, 1971; Vol. 2.

(4) Helenius, A.; Simons, K. Solubilization of Membranes by Detergents. *Biochim. Biophys. Acta, Biomembr.* **1975**, *415*, 29−79.

(5) Reis, S.; Moutinho, C. G.; Matos, C.; de Castro, B.; Gameiro, P.; Lima, J. L. F. C. Non-invasive Methods to Determine the Critical Micelle Concentration of Some Bile Acid Salts. *Anal. Biochem.* **2004**, *334*, 117−126.

(6) Paula, S.; Sues, W.; Tuchtenhagen, J.; Blume, A. Thermodynamics of Micelle Formation as a Function of Temperature: A High Sensitivity Titration Calorimetry Study. *J. Phys. Chem.* **1995**, *99*, 11742−11751.

(7) Kratohvil, J. P. Size of Bile Salt Micelles: Techniques, Problems and Results. *Adv. Colloid Interface Sci.* **1986**, *26*, 131−154.

(8) Hinze, W. L.; Hu, W.; Quina, F. H.; Mohammadzai, I. U. Bile Acid/Salt Surfactant Systems: General Properties and Survey of Analytical Applications. In *Organized Assemblies in Chemical Analysis*; Hinze, W. L., Ed. JAI Press: Stamford, CT, 2000; Vol. 2, pp 1−70.

(9) Mazer, N. A.; Carey, M. C.; Kwasnick, R. F.; Benedek, G. B. Quasielastic Light Scattering Studies of Aqueous Biliary Lipid Systems. Size, Shape, and Thermodynamics of Bile Salt Micelles. *Biochemistry* **1979**, *18*, 3064−3075.

(10) Schurtenberger, P.; Mazer, N.; Kaenzig, W. Static and Dynamic Light Scattering Studies of Micellar Growth and Interactions in Bile Salt Solutions. *J. Phys. Chem.* **1983**, *87*, 308−315.

(11) Galantini, L.; Giglio, E.; Leonelli, A.; Pavel, N. V. An Integrated Study of Small-Angle X-ray Scattering and Dynamic Light Scattering on Cylindrical Micelles of Sodium Glycodeoxycholate. *J. Phys. Chem. B* **2004**, *108*, 3078−3085.

(12) Lopez, F.; Samseth, J.; Mortensen, K.; Rosenqvist, E.; Rouch, J. Micro- and Macrostructural Studies of Sodium Deoxycholate Micellar Complexes in Aqueous Solutions. *Langmuir* **1996**, *12*, 6188−6196.

(13) Mukerjee, P.; Cardinal, J. R. Solubilization as a Method for Studying Self-Association: Solubility of Naphthalene in the Bile Salt Sodium Cholate and the Complex Pattern of its Aggregation. *J. Pharm. Sci.* **1976**, *65*, 882−886.

(14) Li, R.; Carpentier, E.; Newell, E. D.; Olague, L. M.; Heafey, E.; Yihwa, C.; Bohne, C. Effect of the Structure of Bile Salt Aggregates on the Binding of Aromatic Guests and the Accessibility of Anions. *Langmuir* **2009**, *25*, 13800−13808.

(15) Kolehmainen, E.; Laatikainen, R. Solubilization of Aromatics in Aqueous Bile Salts: III. Thermodynamic Model for Solubilization of Benzene in Sodium Cholate Based on ^{1}H NMR Chemical Shifts. *J. Colloid Interface Sci.* **1988**, *121*, 148−153.

(16) Kolehmainen, E. Solubilization of Aromatics in Aqueous Bile Salts: II. Benzene and Some Substituted Benzenes in Sodium Deoxycholate and Cholate: ^{1}H and ^{19}F NMR Studies. *J. Colloid Interface Sci.* **1989**, *127*, 301−309.

(17) Luo, J.; Giguère, G.; Zhu, X. X. Asymmetric Poly(ethylene glycol) Star Polymers with a Cholic Acid Core and Their Aggregation Properties. *Biomacromolecules* **2009**, *10*, 900−906.

(18) Chen, Y.; Luo, J.; Zhu, X. X. Fluorescence Study of Inclusion Complexes between Star-Shaped Cholic Acid Derivatives and Polycyclic Aromatic Fluorescent Probes and the Size Effects of Host and Guest Molecules. *J. Phys. Chem. B* **2008**, *112*, 3402−3409.

(19) Luo, J.; Chen, Y.; Zhu, X. X. Invertible Amphiphilic Molecular Pockets Made of Cholic Acid. *Langmuir* **2009**, *25*, 10913−10917.

(20) Luo, J.; Xiao, K.; Li, Y.; Lee, J. S.; Shi, L.; Tan, Y.-H.; Xing, L.; Holland Cheng, R.; Liu, G.; Lam, K. S. Well-Defined, Size-Tunable, Multifunctional Micelles for Efficient Paclitaxel Delivery for Cancer Treatment. *Bioconjugate Chem.* **2010**, *21*, 1216−1224.

(21) Knop, K.; Hoogenboom, R.; Fischer, D.; Schubert, U. Poly(ethylene glycol) in Drug Delivery: Pros and Cons as Well as Potential Alternatives. *Angew. Chem., Int. Ed.* **2010**, *49*, 6288−6308.

(22) Lutz, J. F. Polymerization of Oligo(ethylene glycol) (meth)-acrylates: Toward New Generations of Smart Biocompatible Materials. *J. Polym. Sci., Part A: Poly. Chem.* **2008**, *46*, 3459−3470.

(23) Merrill, E. W.; Harris, J. M. *Poly(ethylene glycol) Chemistry: Biotechnical and Biomedical Applications*; Springer: New York, 1992; pp 199− 220.

(24) Filpula, D.; Zhao, H. Releasable PEGylation of Proteins with Customized Linkers. *Adv. Drug Delivery Rev.* **2008**, *60*, 29−49.

(25) Kim, I.-S.; Kim, S.-H. Evaluation of Polymeric Nanoparticles Composed of Cholic Acid and Methoxy Poly(ethylene glycol). *Int. J. Pharm.* **2001**, *226*, 23−29.

(26) Torchilin, V. P. PEG-based Micelles as Carriers of Contrast Agents for Different Imaging Modalities. *Adv. Drug Delivery Rev.* **2002**, *54*, 235−252.

(27) Strandman, S.; Le Dévédec, F.; Zhu, X. X. Thermosensitivity of Bile Acid-Based Oligo(ethylene glycol) Stars in Aqueous Solutions. *Macromol. Rapid Commun.* **2011**, *32*, 1185−1189.

(28) Al-Saidan, S. M. Transdermal Self-Permeation Enhancement of Ibuprofen. *J. Controlled Release* **2004**, *100*, 199−209.

(29) Bohne, C.; Redmond, R. W.; Scaiano, J. C. Use of Photophysical Techniques in the Study of Organized Assemblies. In *Photochemistry in Organized and Constrained Media*; Ramamurthy, V., Ed.; VCH Publishers: New York, 1991; pp 79−132.

(30) Gouin, S.; Zhu, X. X. Fluorescence and NMR Studies of the Effect of a Bile Acid Dimer on the Micellization of Bile Salts. *Langmuir* **1998**, *14*, 4025−4029.

(31) Peters, R. *Single-Photon Correlation Techniques. Dynamic Light Scattering: The Method and Some Applications*. Brown, W. Ed.; Clarendon Press: Oxford, U.K., 1993.

(32) Beetge, E.; du Plessis, J.; Müller, D. G.; Goosen, C.; van Rensburg, F. J. The Influence of the Physicochemical Characteristics and Pharmacokinetic Properties of Selected NSAID's on Their Transdermal Absorption. *Int. J. Pharm.* **2000**, *193*, 261−264.

(33) Yiyun, C.; Jiepin, Y. Solubilization of Non-steroidal Anti-inflammatory Drugs in the Presence of Tween Series Surfactants. *Phys. Chem. Liq.* **2006**, *44*, 249 −256.

(34) Egan, R. W. Hydrophile-Lipophile Balance and Critical Micelle Concentration as Key Factors Influencing Surfactant Disruption of Mitochondrial Membranes. *J. Biol. Chem.* **1976**, *251*, 4442−4447.

(35) Umbreit, J. N.; Strominger, J. L. Relation of Detergent HLB Number to Solubilization and Stabilization of D-Alanine Carboxypeptidase from Bacillus subtilis Membranes. *Proc. Natl. Acad. Sci. U.S.A.* **1973**, *70*, 2997−3001.

(36) Kleinman, M. H.; Bohne, C. Use of Photophysical Probes to Study Dynamic Processes in Supramolecular Structures. In *Molecular and Supramolecular Photochemistry*; Ramamurthy, V., Schanze, K. S., Eds.; Marcel Dekker: New York, 1997; Vol. *1*, pp 391−466.

(37) Xu, W.; Demas, J. N.; DeGraff, B. A.; Whaley, M. Interactions of Pyrene with Cyclodextrins and Polymeric Cyclodextrins. *J. Phys. Chem.* **1993**, *97*, 6546−6554.

(38) Kalyanasundaram, K. *Photochemistry in Microheterogeneous Systems*; Academic Press: Orlando, FL, 1987; p 388.

(39) Dong, D. C.; Winnik, M. A. The Py Scale of Solvent Polarities. Solvent Effects of the Vibronic Fine Structure of Pyrene Fluorescence and Empirical Correlations with E_T and Y Values. *Photochem. Photobiol.* **1982**, *35*, 17−21.

(40) Kalyanasundaram, K.; Thomas, J. K. Environmental Effects on Vibronic Band Intensities in Pyrene Monomer Fluorescence and Their Application in Studies of Micellar Systems. *J. Am. Chem. Soc.* **1977**, *99*, 2039−2044.

(41) Sanemasa, I.; Wu, J.-S.; Deguchi, T. A Method for Determining the 1-Octanol/Water Partition Coefficients of Volatile Hydrocarbons. *Anal. Sci.* **1994**, *10*, 655−658.

(42) Fuentealba, D.; Thurber, K.; Bovero, E.; Pace, T. C. S.; Bohne, C. Effect of Sodium Chloride on the Binding of Polyaromatic

Hydrocarbon Guests with Sodium Cholate Aggregates. *Photochem. Photobiol. Sci.* **2011**, *10*, 1420−1430.
(43) Ju, C.; Bohne, C. Probing Bile Salt Aggregates by Fluorescence Quenching. *Photochem. Photobiol.* **1996**, *63*, 60−67.
(44) Yihwa, C.; Bohne, C. Effect of Solvent Polarity and Viscosity on the Guest Binding Dynamics with Bile Salt Aggregates. *Photochem. Photobiol.* **2007**, *83*, 494−502.
(45) Yihwa, C.; Kellermann, M.; Becherer, M.; Hirsch, A.; Bohne, C. Pyrene Binding to Persistent Micelles Formed from a Dendro-Calixarene. *Photochem. Photobiol. Sci.* **2007**, *6*, 525−531.
(46) Matsuoka, K.; Moroi, Y. Micelle Formation of Sodium Deoxycholate and Sodium Ursodeoxycholate (Part 1). *Biochim. Biophys. Acta* **2002**, *1580*, 189−199.
(47) Matsuzaki, K.; Yokoyama, I.; Komatsu, H.; Handa, T.; Miyajima, K. A Fluorescent Probing Study on Microenvironments in Bile Salt Micelles and Bile Salt/Phosphatidylcholine Mixtures in the Absence or Presence of Cholesterol. *Biochim. Biophys. Acta* **1989**, *980*, 371−376.
(48) Zana, R.; Guveli, D. Fluorescence Probing Study of the Association of Bile Salts in Aqueous Solutions. *J. Phys. Chem.* **1985**, *89*, 1687−1690.
(49) Jover, A.; Meijide, F.; Rodríguez Núñez, E.; Vázquez Tato, J. Unusual Pyrene Excimer Formation during Sodium Deoxycholate Gelation. *Langmuir* **1996**, *12*, 1789−1793.
(50) Montalti, M.; Credi, A.; Prodi, L.; Gandolfi, M. T. *Handbook of Photochemistry*, 3rd ed.; CRC Press: Boca Raton, FL, 2006.
(51) Amundson, L. L.; Li, R.; Bohne, C. Effect of the Guest Size and Shape on Its Binding Dynamics with Sodium Cholate Aggregates. *Langmuir* **2008**, *24*, 8491−8500.
(52) Li, R.; Santos, C. S.; Norsten, T. B.; Morimitsu, K.; Bohne, C. Aqueous Solubilization of Photochromic Compounds by Bile Salt Aggregates. *Chem. Commun.* **2010**, *46*, 1941−1943.
(53) Pace, T. C. S.; Souza Júnior, S. P.; Zhang, H. T.; Bohne, C. Effect of Terbium(III) on the Binding of Aromatic Guests with Sodium Taurocholate Aggregates. *Photochem. Photobiol. Sci.* **2011**, *10*, 1568−1577.
(54) Chen, M.; Grätzel, M.; Thomas, J. K. Kinetic Studies in Bile Acid Micelles. *J. Am. Chem. Soc.* **1975**, *97*, 2052−2057.